Int. J. of Applied Mechanics and Engineering, 2006, vol.11, No.3, pp.679-698

NONLINEAR STATIC AND DYNAMIC ANALYSIS OF FUNCTIONALLY GRADED PLATES

Tsung-Lin WU
Automative Division of Mechanical Engineering Department
Southern Taiwan University of Technology
Tainan, Taiwan 701, REPUBLIC OF CHINA

K.K. SHUKLA
Department of Applied Mechanics, M.N.N.I.T. Allahabad 04
INDIA

Jin. H. HUANG*
Department of Mechanical and Computer-Aided Engineering
Feng Chia University
Taichung 407, TAIWAN
e-mail: jhhuang@fcu.edu.tw

An explicit solution for the nonlinear static and dynamic responses of the functionally graded materials rectangular plate is obtained. The volume fraction of the material constituents is assumed to follow a simple power law distribution. The formulation is based on the first-order shear deformation theory and von-Karman nonlinear kinematics. The solution methodology utilizes the quadratic extrapolation technique for linearization, finite double Chebyshev series for spatial discretization of the variables and Houbolt time marching scheme for temporal discretization. Numerical results show the effect of volume fraction exponent of the constituent materials on the nonlinear static and dynamic responses of the plate with different boundary conditions and plate span to thickness ratio. Analysis results indicate that the effect of the volume fraction exponent *n* up to two on the displacement of the plate is more significant.

Key words: functionally graded materials, nonlinear static and dynamic response, Chebyshev polynomial.

1. Introduction

Thin and moderately thick plates/panels are one of the major load bearing structural elements in high performance engineering structures. Fiber composite laminated plates are widely used in structures such as space structures, nuclear reactor vessels, automobiles, turbines etc. They are usually subjected to severe non-uniform thermomechanical loading conditions during their service life. The failures of these components are mainly due to the large amplitude of vibrations under transient loading, buckling or excessive stresses and deformations induced by thermo-mechanical loadings. The fiber composite laminated plates/panels show destabilizing effect at elevated temperature as the material properties such as the modulus of elasticity reduces considerably at higher temperature. Also the exact analyses of laminated fiber composites are difficult due to the presence of a large number of interfaces between the layers. Recent studies on a new performance material known as functionally graded materials (FGM's) reveal that these materials are suitable for structures exposed to non-uniform service conditions and under high thermal environment. The functionally graded materials are microscopically heterogeneous and made from isotropic materials such as metals and ceramics. In functionally graded materials, the material properties are graded continuously and

* To whom correspondence should be addressed

vary smoothly from one surface to another and thus the disadvantage of interfaces in the laminated composites are eliminated.

The nonlinear static and dynamic analyses of isotropic and fiber reinforced composite laminated plates have been carried out by many investigators using an analytical approach, mainly employing generalized Fourier series and finite element based numerical tools. A detailed comprehensive review of the problems related to the geometric nonlinear analysis of composite plates and nonlinear vibration of plates using analytical and finite elements methods are presented by Chia (1988) and Sathyamoorthy (1987), respectively. Tauchert (1991) presented a classical review of the flexure, buckling and vibration of plates due to thermal loading. It can be seen from the literature that considerable efforts are made for the analysis of the composite laminated plates/panels.

In recent years the functionally graded materials have found increased applications in advanced engineering structures which are exposed to high temperature environment, since they were first reported in 1984 in Japan (Koizumi, 1993). The analyses of the functionally graded materials plates/panels have received considerable attention of the researchers in recent past. Finot and Suresh (1996) presented a closed form solution based on the classical Kirchhoff's theory of thin plates for the analysis of multilayered and functionally graded material plates, subjected to thermal loading. The dynamic thermoelastic response of the functionally graded cylinders and plates are obtained by Reddy and Chin (1998). Praveen and Reddy (1998) obtained the nonlinear transient thermoelastic response of the functionally graded ceramic metal plates using a plate finite element method, employing transverse shear strain, rotary inertia and von-Karman nonlinearity. Loy *et al.* (1999) presented a free vibration analysis of simply supported FGM thin cylindrical shells. Pradhan *et al.* (2000) presented the solution for free vibration of FGM cylindrical thin shells for different boundary conditions. Reddy (2000) obtained the Navier's solution of rectangular FGM plate using finite element based models and incorporating third order shear deformation theory and von-Karman type nonlinearity. Zhong and Shang (2003) obtained three-dimensional analytical solutions for a simply supported functionally gradient piezoelectric plate. Employing classical nonlinear von-Karman plate theory, Ma and Wang (2003) investigated axisymmetric large deflection analysis of a functionally graded circular plate. Vel and Batra (2002, 2003) presented an analytical solution for the three dimensional analysis of simply supported functionally graded rectangular plate subjected to thermal and mechanical loadings. Yang and Shen (2003) presented a semi-numerical approach for the nonlinear bending analysis of the shear deformable functionally graded rectangular plate subjected to thermo-mechanical loading. From the available literature, it is evident that less attention has been paid to the nonlinear analysis of the functionally graded plates and analytical solutions to the nonlinear static and dynamic responses of the FGM plates are a few. In order to have the reliable service and lifetime prediction of the FGM plates, it is necessary to clearly examine the nonlinear response of the FGM plates under different loading conditions, so that the influence of the graded material properties can be understood thoroughly. Hence, there is a need to obtain the nonlinear response of the FGM plates, analytically, in order to have a better understanding of their behavior.

In the present paper, an attempt is made to obtain the analytical-numerical type solution for the nonlinear static and dynamic responses of the moderately thick functionally graded materials plates. The present methodology of the solution is based on the fast converging finite double Chebyshev series, which can be used for plates with different boundary conditions. The mathematical formulation is based on first-order shear deformation theory and von-Karman nonlinear kinematics. The properties of the plate are considered to vary across the thickness of the plate according to power law. The effects of volume fraction of the material constituents on the nonlinear static and dynamic displacement responses of the FGM plate with different combinations of the boundary conditions and plate span to thickness ratio are investigated.

2. Problem formulation

2.1. Functionally graded material plates

Functionally graded materials are composite and microscopically inhomogeneous with mechanical and thermal properties varying smoothly and continuously from one surface to the other. These materials are

made from a mixture of ceramics and metals or combination of different metals by gradually varying the volume fraction of the constituent metals. The properties of the plate are assumed to vary through the thickness of the plate. A simple rule of a mixture based on power law is used to obtain the effective properties of an FGM plate of thickness h shown in Fig.1. The effective properties of the FGM plate can be written as (Praveen and Reddy, 1998)

$$E(z) = E_m + (E_c - E_m)\left(\frac{2z+h}{2h}\right)^n, \tag{2.1}$$

$$\rho(z) = \rho_m + (\rho_c - \rho_m)\left(\frac{2z+h}{2h}\right)^n \tag{2.2}$$

where E_c, ρ_c and E_m, ρ_m are the corresponding properties of the ceramic and metals, z is the thickness coordinate $(-h/2 \le z \le h/2)$, and n is the volume fraction exponent which takes values greater than or equal to zero. The value of $n=1$, indicates the linear variation of the composition of the materials through the thickness and $n=0$ represents a fully ceramic plate. The Poisson's ratio is assumed to be constant for both the materials.

$$\nu(z) = \nu\,. \tag{2.3}$$

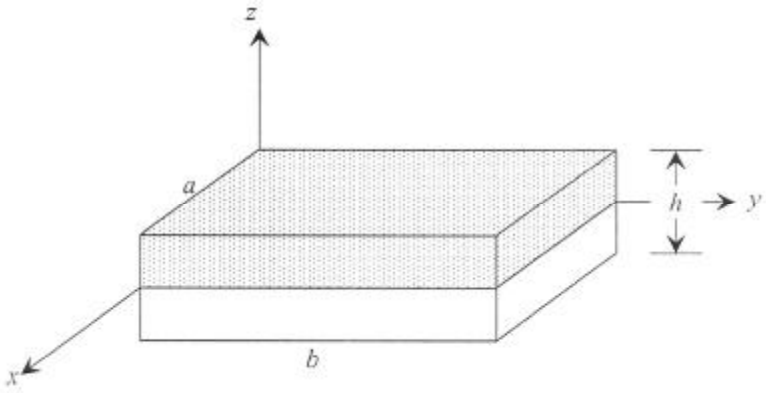

Fig.1. Geometry of the FGM plate.

2.2. Governing equations of motion

A rectangular plate of dimensions a, b, and h shown in Fig.1, is considered for the analysis. Based on the first-order shear deformation theory, the displacement field at a point in the plate is expressed as

$$\begin{aligned} U(x, y, z, t) &= u_0(x, y, t) + z\theta_x(x, y, t), \\ V(x, y, z, t) &= v_0(x, y, t) + z\theta_y(x, y, t), \\ W(x, y, z, t) &= w_0(x, y, t) \end{aligned} \tag{2.4}$$

where u_0, v_0 and w_0 are the displacements at a point on the mid-plane of the plate in *x*, *y* and *z* directions, respectively. θ_x and θ_y are the rotations of *yz* and *xz* planes of the plate, respectively.

Employing the von-Karman nonlinearity, which takes into account moderately large deformations and small strains, the strain-displacement relations are expressed as

$$\begin{Bmatrix} \varepsilon_x \\ \varepsilon_y \\ \gamma_{xy} \\ \gamma_{yz} \\ \gamma_{xz} \end{Bmatrix} = \begin{Bmatrix} u_{0,x} + \frac{1}{2}(w_{0,x})^2 \\ v_{0,y} + \frac{1}{2}(w_{0,y})^2 \\ u_{0,y} + v_{0,x} + w_{0,x} w_{0,y} \\ w_{0,y} + \theta_y \\ w_{0,x} + \theta_x \end{Bmatrix} + z \begin{Bmatrix} \theta_{x,x} \\ \theta_{y,y} \\ \theta_{x,y} + \theta_{y,x} \\ 0 \\ 0 \end{Bmatrix}. \tag{2.5}$$

The constitutive equations for the FGM plate with plane stress condition and transverse shear is given by

$$\begin{Bmatrix} \sigma_x \\ \sigma_y \\ \tau_{xy} \\ \tau_{yz} \\ \tau_{xz} \end{Bmatrix} = \begin{bmatrix} Q_{11} & Q_{12} & 0 & 0 & 0 \\ Q_{12} & Q_{22} & 0 & 0 & 0 \\ 0 & 0 & Q_{66} & 0 & 0 \\ 0 & 0 & 0 & Q_{44} & 0 \\ 0 & 0 & 0 & 0 & Q_{55} \end{bmatrix} \begin{Bmatrix} \varepsilon_x \\ \varepsilon_y \\ \gamma_{xy} \\ \gamma_{yz} \\ \gamma_{xz} \end{Bmatrix}. \tag{2.6}$$

The in-plane force and moment resultants of the plate are expressed as

$$\begin{Bmatrix} N_x \\ N_y \\ N_{xy} \\ M_x \\ M_y \\ M_{xy} \end{Bmatrix} = \begin{bmatrix} A_{11} & A_{12} & 0 & B_{11} & B_{12} & 0 \\ A_{12} & A_{22} & 0 & B_{12} & B_{22} & 0 \\ 0 & 0 & A_{66} & 0 & 0 & B_{66} \\ B_{11} & B_{12} & 0 & D_{11} & D_{12} & 0 \\ B_{12} & B_{22} & 0 & D_{12} & D_{22} & 0 \\ 0 & 0 & B_{66} & 0 & 0 & D_{66} \end{bmatrix} \begin{Bmatrix} u_{0,x} + \frac{1}{2}(w_{0,x})^2 \\ v_{0,y} + \frac{1}{2}(w_{0,y})^2 \\ u_{0,y} + v_{0,x} + w_{0,x} w_{0,y} \\ \theta_{x,x} \\ \theta_{y,y} \\ \theta_{x,y} + \theta_{y,x} \end{Bmatrix}. \tag{2.7}$$

The transverse shear forces are expressed as

$$\begin{Bmatrix} Q_y \\ Q_x \end{Bmatrix} = \begin{bmatrix} A_{44} & 0 \\ 0 & A_{55} \end{bmatrix} \begin{Bmatrix} w_{0,y} + \theta_y \\ w_{0,x} + \theta_x \end{Bmatrix} \tag{2.8}$$

where stiffness coefficients $A_{ij}, B_{ij}, D_{ij}\ (i, j = 1, 2, 6)$ and $A_{ij}\ (i, j = 4, 5)$ are in-plane, bending-stretching coupling, bending, and thickness shear stiffnesses, respectively and are defined in terms of Q_{ij} as

$$\left(A_{ij}, B_{ij}, D_{ij}\right) = \int_{-h/2}^{h/2} \left\{\left(Q_{ij}^c - Q_{ij}^m\right)\left(\frac{2z+h}{2h}\right)^n + Q_{ij}^m\right\}\left(1, z, z^2\right)dz \qquad (i, j = 1, 2, 4, 5, 6) \qquad (2.9)$$

where

$$Q_{11}^m = Q_{22}^m = \frac{E_m}{1-\nu^2}, \quad Q_{12}^m = \frac{\nu E_m}{1-\nu^2}, \quad Q_{44}^m = Q_{55}^m = Q_{66}^m = \frac{E_m}{2(1+\nu)} \qquad \text{for metals,}$$

$$Q_{11}^c = Q_{22}^c = \frac{E_c}{1-\nu^2}, \quad Q_{12}^c = \frac{\nu E_c}{1-\nu^2}, \quad Q_{44}^c = Q_{55}^c = Q_{66}^c = \frac{E_c}{2(1+\nu)} \qquad \text{for ceramic.}$$

Equation (2.9) is further simplified and the expressions for plate stiffnesses may be written as

$$A_{ij} = \left(Q_{ij}^c - Q_{ij}^m\right)\left(\frac{h}{n+1}\right) + Q_{ij}^m h, \qquad (2.10a)$$

$$B_{ij} = \left(Q_{ij}^c - Q_{ij}^m\right)\left\{\frac{nh^2}{2(n+1)(n+2)}\right\}, \qquad (2.10b)$$

$$D_{ij} = \left(Q_{ij}^c - Q_{ij}^m\right)\left\{\frac{\left(2+n+n^2\right)h^3}{4(n+1)(n+2)(n+3)}\right\} + Q_{ij}^m \frac{h^3}{12}. \qquad (2.10c)$$

The governing equations of motion are derived using Hamilton's principle and are expressed in a non-dimensional form as

$$\left(\boldsymbol{L}_a + \boldsymbol{L}_b + \boldsymbol{L}_c\right)\boldsymbol{d} + \boldsymbol{q} = \boldsymbol{L}_\tau \boldsymbol{d} \qquad (2.11)$$

where

$$\boldsymbol{L}_a = \boldsymbol{L}_{a1}\frac{\partial^2}{\partial x^2} + \boldsymbol{L}_{a2}\frac{\partial^2}{\partial y^2} + \boldsymbol{L}_{a3}\frac{\partial^2}{\partial x \partial y} + \boldsymbol{L}_{a4}\frac{\partial}{\partial x} + \boldsymbol{L}_{a5}\frac{\partial}{\partial y} + \boldsymbol{L}_{a6},$$

$$\boldsymbol{L}_b = \boldsymbol{L}_{b1}\frac{\partial^2}{\partial x^2} + \boldsymbol{L}_{b2}\frac{\partial^2}{\partial y^2} + \boldsymbol{L}_{b3}\frac{\partial^2}{\partial x \partial y},$$

$$\boldsymbol{L}_c = \boldsymbol{L}_{c1}\frac{\partial^2}{\partial x^2} + \boldsymbol{L}_{c2}\frac{\partial^2}{\partial y^2} + \boldsymbol{L}_{c3}\frac{\partial^2}{\partial x \partial y},$$

$$\boldsymbol{L}_\tau = \boldsymbol{L}_{\tau 1}\frac{\partial^2}{\partial \tau^2},$$

$$\boldsymbol{d} = \left[u \;\; v \;\; w \;\; \theta_x \;\; \theta_y\right]^T,$$

$$\boldsymbol{q} = \left[0 \;\; 0 \;\; q_z \;\; 0 \;\; 0\right]^T.$$

The matrices $\boldsymbol{L}_{a1} \sim \boldsymbol{L}_{a6}$, $\boldsymbol{L}_{b1} \sim \boldsymbol{L}_{b3}$, $\boldsymbol{L}_{c1} \sim \boldsymbol{L}_{c3}$ and $\boldsymbol{L}_{\tau 1}$ are given in the Appendix.

2.3. Boundary conditions

The boundary conditions along with the governing equations are obtained and either displacement or traction is prescribed at the boundaries. The following boundary conditions are considered for clamped (C) and simply supported (S) boundary conditions at the edges of the plate.

Clamped (C): $u_0 = 0$, $v_0 = 0$, $w_0 = 0$, $\theta_x = 0$, $\theta_y = 0$ at all the edges

Simply Supported (S): $u_0 = 0$, $v_0 = 0$, $w_0 = 0$, $M_x = 0$, $\theta_y = 0$ at $x = \pm a/2$

$u_0 = 0$, $v_0 = 0$, $w_0 = 0$, $\theta_x = 0$, $M_y = 0$ at $y = \pm b/2$

3. Analytical methodology of solution

The nonlinear analysis of isotropic, orthotropic and laminated plates has been carried out analytically by many investigators (Chia, 1988). In most of the studies, Fourier series is used and Levy-type solution is obtained. In the present paper, finite double Chebyshev series is employed for the solution, which can also be used for solving plates with non-Levy type boundary conditions. The Chebyshev polynomials have been used for solving the boundary value problems and some of them are due to Evans and Murphy (1981), Nath and Shukla (2001), Lin and Jen (2003), and Shukla *et al.* (2004).

The displacement functions and the loading is approximated in space domain by finite degree double Chebyshev polynomials (Fox and Parker, 1968) as

$$\xi(x, y) = \sum_{i=0}^{M}\sum_{j=0}^{M} \delta_{ij}\xi_{ij}T_i(x)T_j(y) \tag{3.1}$$

where

$$\delta_{00} = 0.25,$$

$$\delta_{i0} = \delta_{0j} = 0.5,$$

$$\delta_{ij} = 1;\ i, j \neq 0.$$

The spatial derivative of the function $\xi(x, y)$ is expressed as

$$\xi^{rs}_{,xy} = \sum_{i=0}^{M-r}\sum_{j=0}^{N-s} \delta_{ij}\xi^{rs}_{ij}T_i(x)T_j(y) \tag{3.2}$$

where *r* and *s* are the order of derivatives with respect to *x* and *y*, respectively, and the function $\xi(x, y)$ is in the range of $-1 \le x \le 1$ and $-1 \le y \le 1$. The derivative function ξ_{ij}^{rs} is evaluated, using the recurrence relations given as (Fox and Parker, 1968)

$$\begin{aligned} \xi_{(i-1)j}^{rs} &= \xi_{(i+1)j}^{rs} + 2i\xi_{ij}^{(r-1)s}, \\ \xi_{i(j-1)}^{rs} &= \xi_{i(j+1)}^{rs} + 2j\xi_{ij}^{r(s-1)}. \end{aligned} \tag{3.3}$$

The nonlinear terms which are the product of the displacement functions or their derivatives in the governing Eq.(2.11) are predicted at every step of marching variable (load) using quadratic extrapolation technique and added to the load vector. A typical nonlinear function ζ at step *J* is expressed as

$$\zeta_j = \left[\sum_{i=0}^{M-r}\sum_{j=0}^{N}\delta_{ij}\xi_{ij}^{r}T_i(x)T_j(y)\right]_J \times \left[\sum_{i=0}^{M}\sum_{j=0}^{N-s}\delta_{ij}\xi_{ij}^{s}T_i(x)T_j(y)\right]_J \tag{3.4}$$

where

$$\left(\xi_{ij}\right)_J = A_1\left(\xi_{ij}\right)_{J-1} + A_2\left(\xi_{ij}\right)_{J-2} + A_3\left(\xi_{ij}\right)_{J-3}. \tag{3.5}$$

During initial steps of marching variables, the coefficients A_1, A_2 and A_3 of the quadratic extrapolation scheme of linearization takes the following values

$$1, 0, 0\,(J=1); \quad 2, -1, 0\,(J=2); \quad 3, -3, 1\,(J \ge 3).$$

The product of two Chebyshev polynomials is expressed as

$$\begin{aligned} T_i(x)T_j(y)T_k(x)T_m(y) = \frac{1}{4}\big[&T_{i+k}(x)T_{j+m}(y) + T_{i+k}(x)T_{j-m}(y) + \\ &+ T_{i-k}(x)T_{j+m}(y) + T_{i-k}(x)T_{j-m}(y)\big]. \end{aligned} \tag{3.6}$$

For temporal discretization of the displacement terms, appearing in the governing equations, implicit Houbolt time-marching scheme (Houbolt, 1950) is used. The acceleration terms $u_{,\tau\tau}$, $v_{,\tau\tau}$, $w_{,\tau\tau}$, $\theta_{x,\tau\tau}$ and $\theta_{y,\tau\tau}$ in the governing equations are evaluated at each time step and added to the load vector. At any time step *J*, the general acceleration $\left(\xi_{,\tau\tau}\right)_J$ is evaluated as

$$\left(\xi_{,\tau\tau}\right)_J = \left(\beta_1\xi_J + \beta_2\xi_{J-1} + \beta_3\xi_{J-2} + \beta_4\xi_{J-3} + \beta_5\right)/\left(\Delta\tau^2\right). \tag{3.7}$$

The Houbolt acceleration coefficients for step function load is given as

$$\beta_1 = 6, \quad \beta_2 = 0, \quad \beta_3 = 0, \quad \beta_4 = 0, \quad \beta_5 = -2Q^*\Delta\tau^2 \quad \text{for} \quad J = 1,$$

$$\beta_1 = 2, \quad \beta_2 = -4, \quad \beta_3 = 0, \quad \beta_4 = 0, \quad \beta_5 = -Q^*\Delta\tau^2 \quad \text{for} \quad J = 2,$$

$$\beta_1 = 2, \quad \beta_2 = -5, \quad \beta_3 = 4, \quad \beta_4 = 0, \quad \beta_5 = 0 \qquad \text{for} \quad J = 3,$$

$$\beta_1 = 2, \quad \beta_2 = -5, \quad \beta_3 = 4, \quad \beta_4 = -1, \quad \beta_5 = 0 \qquad \text{for} \quad J \geq 3,$$

where Q^* is the non-dimensional uniform step load and τ is the non-dimensional time.

The procedures described above are used for spatial and temporal discretization and linearization of the terms appearing in the governing nonlinear coupled partial differential equations. The governing nonlinear differential equations are linearized and discretized in space and time domain and after collocating the zeroes of the Chebyshev polynomials reduced to a set of simultaneous linear algebraic equations, which are expressed as

$$\sum_{i=0}^{M-2}\sum_{j=0}^{N-2} f_1\left(u_{ij}, \nu_{ij}, w_{ij}, \theta_{xij}, \theta_{yij}, \overline{Q}_{ij}\right) T_i(x) T_j(y) = 0, \tag{3.8a}$$

$$\sum_{i=0}^{M-2}\sum_{j=0}^{N-2} f_2\left(u_{ij}, \nu_{ij}, w_{ij}, \theta_{xij}, \theta_{yij}, \overline{Q}_{ij}\right) T_i(x) T_j(y) = 0, \tag{3.8b}$$

$$\sum_{i=0}^{M-2}\sum_{j=0}^{N-2} f_3\left(u_{ij}, \nu_{ij}, w_{ij}, \theta_{xij}, \theta_{yij}, \overline{Q}_{ij}\right) T_i(x) T_j(y) = 0, \tag{3.8c}$$

$$\sum_{i=0}^{M-2}\sum_{j=0}^{N-2} f_4\left(u_{ij}, \nu_{ij}, w_{ij}, \theta_{xij}, \theta_{yij}, \overline{Q}_{ij}\right) T_i(x) T_j(y) = 0, \tag{3.8d}$$

$$\sum_{i=0}^{M-2}\sum_{j=0}^{N-2} f_5\left(u_{ij}, \nu_{ij}, w_{ij}, \theta_{xij}, \theta_{yij}, \overline{Q}_{ij}\right) T_i(x) T_j(y) = 0 \tag{3.8e}$$

where $\overline{Q}_{ij}$ are the Chebyshev coefficients of the modified load vector Q^*, including the external load, nonlinear terms, and inertia terms.

From Eqs (3.8a) to (3.8e), total $5(M-1)(N-1)$ algebraic equations are generated. Similarly, the boundary conditions are discretized and each clamped edge (C) generates $5M+5$ or $5N+5$ algebraic equations and each simply supported edge (S) generates $5M+4$ or $5N+4$ algebraic equations. So, in case of an FGM plate with all edges clamped (CCCC), the total number of linear algebraic equations become $5(M+1)(N+1)+20$ which are more than the total number of unknown coefficients $5(M+1)(N+1)$. Similar is the case for other boundary conditions such as three edges clamped and one simply supported (CCCS), two opposite edges clamped and two simply supported (CCSS), and two adjacent edges clamped and two simply supported (CSCS). Finally, the discretized linear simultaneous algebraic equations are written in the matrix form as

$$\boldsymbol{A}\boldsymbol{d} = \boldsymbol{Q}^* \tag{3.9}$$

where $\boldsymbol{A}$ is the coefficient matrix, obtained using the spatial and temporal discretization, $\boldsymbol{d}$ is the vector containing the unknown coefficients d_{ij} of the displacements u, ν, w, θ_x and θ_y, and $\boldsymbol{Q}^*$ is the modified load vector consisting of the applied loading, nonlinear terms and inertia terms. The vector $\boldsymbol{Q}^*$ is modified at every iteration across each step.

In the present formulation, the total number of equations becomes greater than the unknown coefficients and hence in order to have a unique and compatible solution, the multiple regression analysis (Shukla *et al.*, 2004) based on the least-square error norms is used, which converts Eq.(3.9) in the following form

$$\boldsymbol{d} = \left(\boldsymbol{A}^T \boldsymbol{A}\right)^{-1} \boldsymbol{A}^T \boldsymbol{Q}^* . \tag{3.10}$$

Solving Eq.(3.10), the unknown coefficients d_{ij} of the displacements are obtained and using Eq.(3.1), the value of the displacement at any point in mid-plane of the plate is obtained.

4. Numerical results and discussions

The nonlinear static and dynamic analysis of the functionally graded materials plate consisting of aluminum and alumina is carried out by utilizing double Chebyshev polynomials. The non-dimensional load and time are incremented in small steps of $\Delta Q^* = 1$ and $\Delta\tau = 0.1$, respectively, using an iterative incremental approach. A relative convergence of *0.1%* of each displacement coefficients d_{ij} at every iteration across each load or time step is adopted. Nine terms expansion of the variables (displacement and load) in Chebyshev series are used for spatial discretization. To ensure the validity of the present solution methodology, the nonlinear static results for transverse central displacement, moment at center and in-plane force at center for clamped isotropic square plate $(a/h = 10)$ under uniform lateral pressure are obtained and compared with the results due to Turvey and Osman (1990). The comparisons for nondimensional central displacement $w_c (= w_0/h)$, central moment $M_x^* \left(= \dfrac{M_x a^2}{Eh^4}\right)$ and in-plane force $N_x^* \left(= \dfrac{N_x a^2}{Eh^3}\right)$ at center are shown in Figs 2-4, respectively. It can be seen that there is good agreement among the results and differences are within less than *3%*, which may be attributed to different solution methodology.

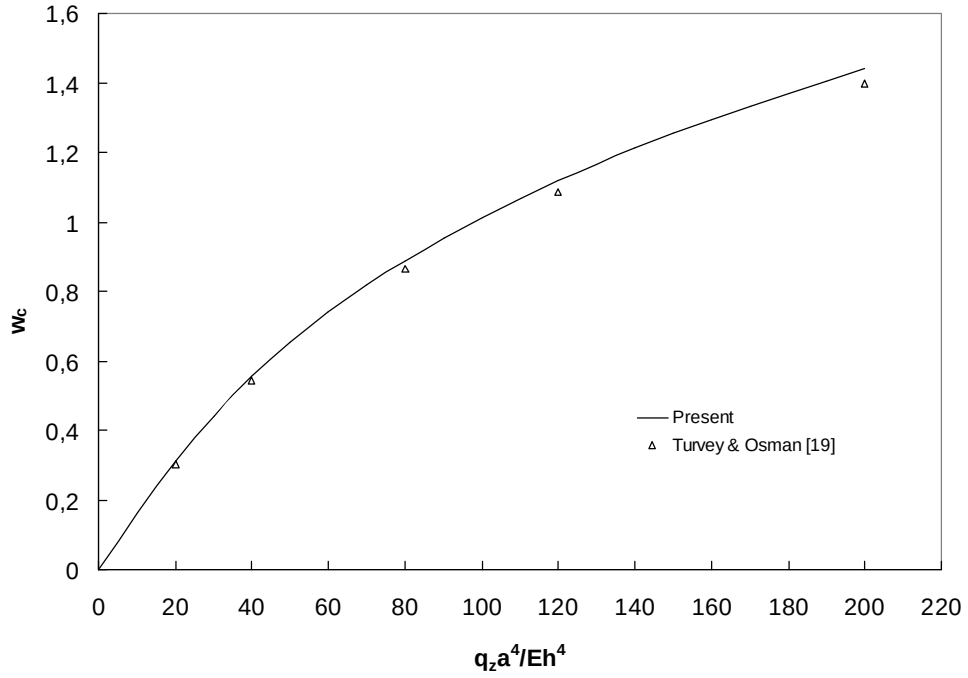

Fig.2. Comparison of the nonlinear static transverse central deflection w_c for a clamped isotropic plate.

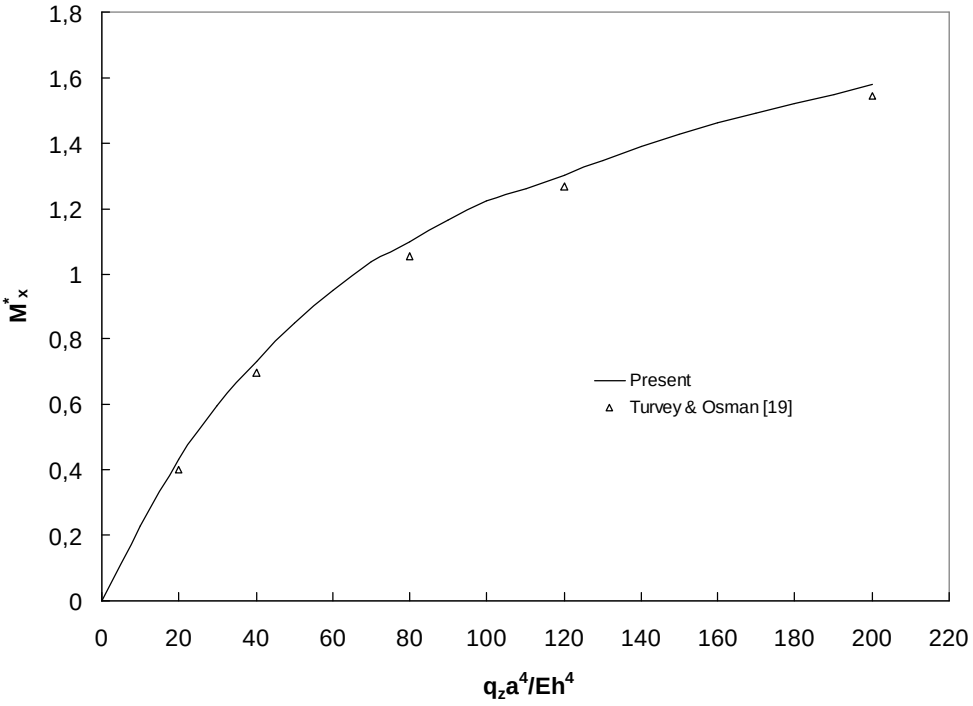

Fig.3. Comparison of moment M_x^* at center for a clamped isotropic plate.

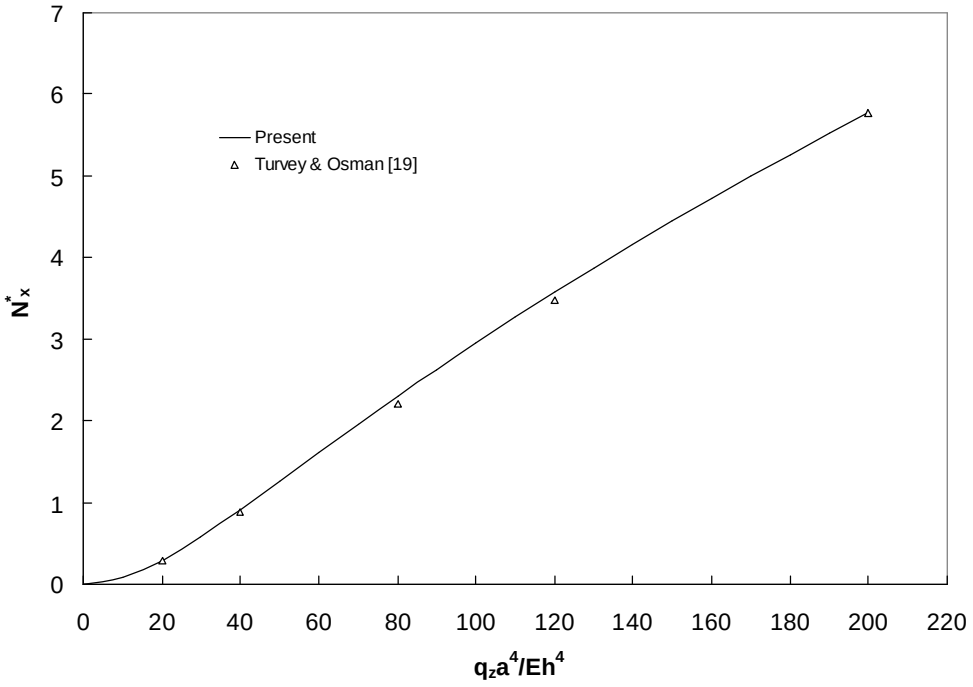

Fig.4. Comparison of in-plane force N_x^* at the center for a clamped isotropic plate.

The numerical results showing the effects of composition of the aluminum and alumina in the plate, plate span to thickness ratio a/h and different boundary conditions on the transverse central displacement are presented. Following material properties are taken in the analysis:

Aluminum: $E_m = 70GPa$, $\nu = 0.3$, and $\rho_m = 2707 kg/m^3$, Alumina: $E_c = 380GPa$, $\nu = 0.3$, and $\rho_c = 3800 kg/m^3$.

The non-dimensionalized parameters used are central deflection $w_c = w_0/h$, transverse load $Q^* = \frac{q_z a^4}{E_m h^4}$, moment at center $M_x^* = \frac{M_x a^2}{D_{11} h}$ and other non-dimensional parameters are shown in the Appendix.

The effect of volume fraction exponent *n* for aluminum and alumina in the plate on the static nonlinear transverse central displacement response of the square moderately thick $(a/h = 10)$ FGM plate with all edges clamped are shown in Fig.5. It is observed that the central displacement is lowest for the alumina plate and highest for aluminum one. It is obvious as the stiffness of alumina is higher than aluminum. With an increase in the value of volume fraction *n*, the central displacement increases. Figure 6 depicts the effect of the volume fraction *n* on the central displacement response for a thin $(a/h = 100)$ CCCC plate. The effects are almost similar as obtained in for a moderately thick plate, which are shown in Fig.5. The variation of the transverse central displacement with volume fraction exponent *n* is shown in Fig.7 for a moderately thick $(a/h = 10)$ clamped plate. It can be observed that the curve between central displacement and volume fraction exponent is almost bilinear. It shows that the effect of volume fraction exponent on transverse central displacement is more pronounced up to $n = 2$ and thereafter its effect diminishes, which can be used as one of the guiding factor in the design of FGM plates.

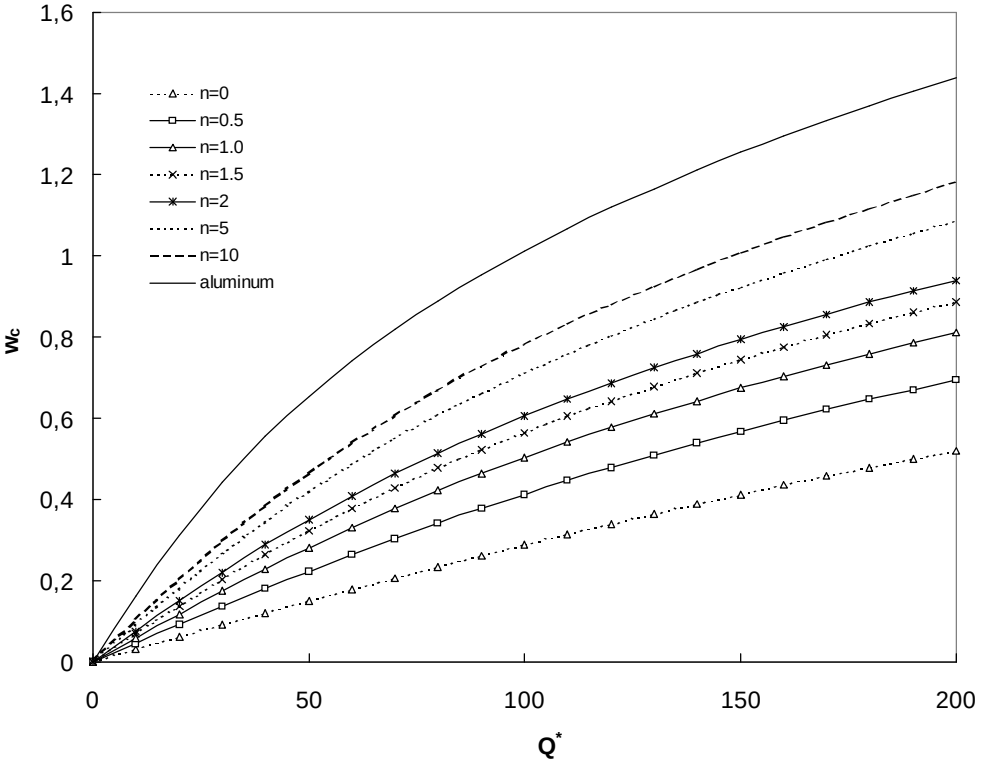

Fig.5. Effect of volume fraction exponent *n* on static transverse deflection of the clamped FGM plate $(a/h = 10)$ under uniform lateral loading.

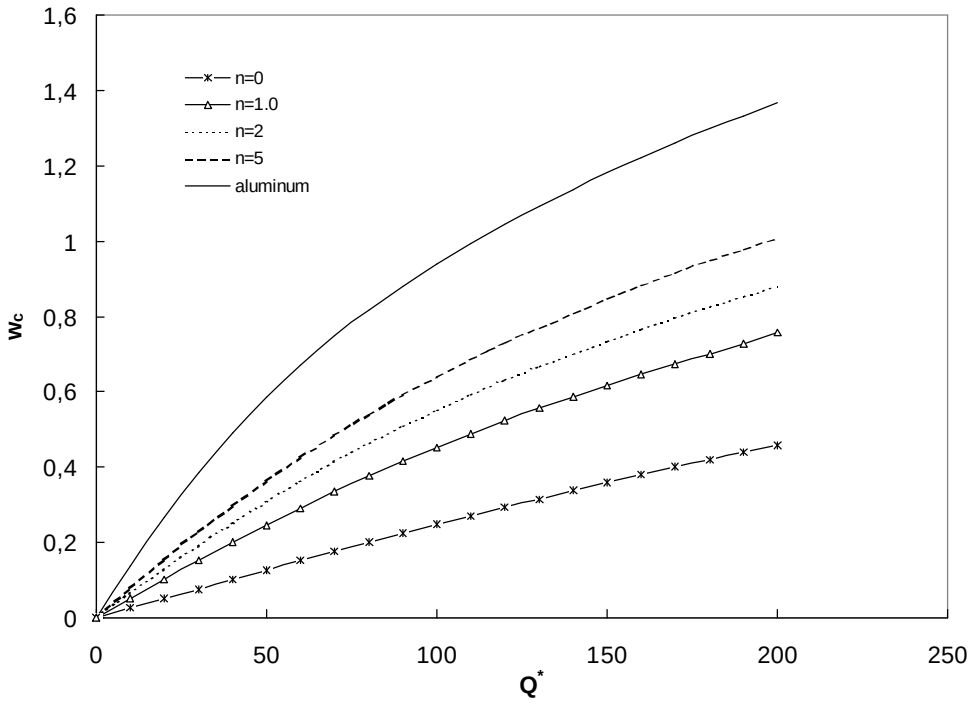

Fig.6. Effect of volume fraction exponent n on static transverse deflection of the clamped FGM plate $(a/h=10)$ under uniform lateral loading.

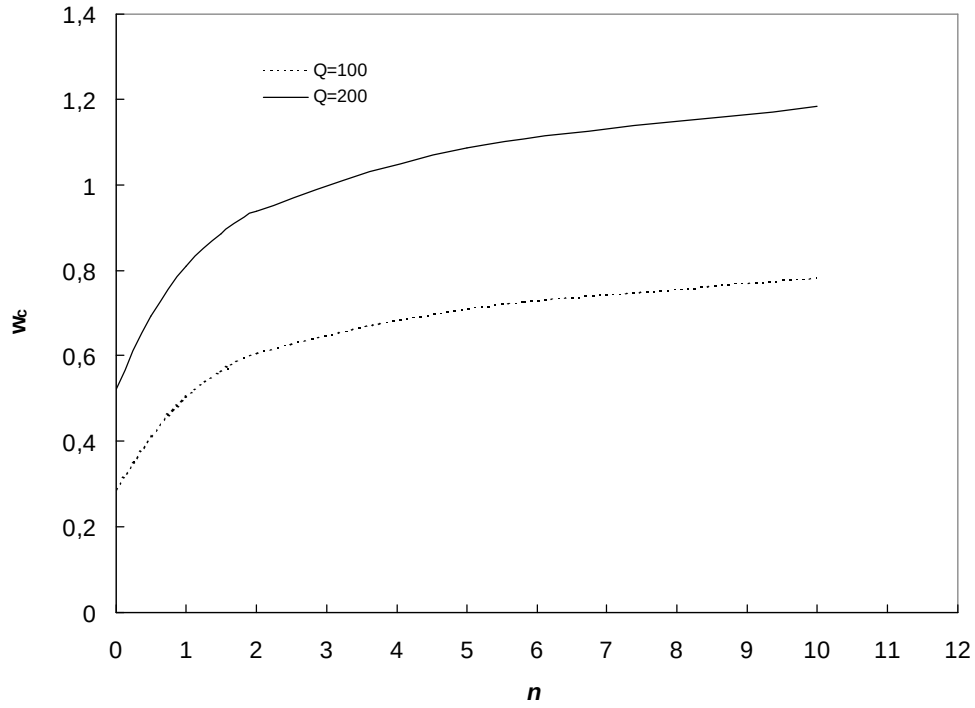

Fig.7. Variation of central deflection w_c with volume fraction exponent n for the clamped FGM plate $(a/h=10)$.

The effects of boundary conditions on the central transverse displacement for a moderately thick $(a/h=20)$ FGM square plate with n equal to 0 and 5, are shown in Fig.8. The figure shows that displacement is lowest for a plate with all edges clamped (CCCC) when the plate is made of alumina or when it is the composition of alumina and aluminum both with volume fraction exponent equal to 5. However, in case of plates with two opposite edges clamped and two simply supported (CCSS) and two adjacent edges clamped and two simply supported (CSCS), the deflection for the CSCS plate is slightly higher than the CCSS plate when $n=0$ i.e., for the plate made of Alumina only. But, for the FGM plate with $n=5$, the displacement in both the cases of boundary conditions CCSS and CSCS is almost same. It is slightly less in case of the CCSS plate when the non-dimensional lateral pressure Q^* is less than 120 but it becomes slightly higher for the CCSS plate when Q^* is greater than 160. For all the boundary conditions, the central displacement increases with an increase in the volume fraction exponent n.

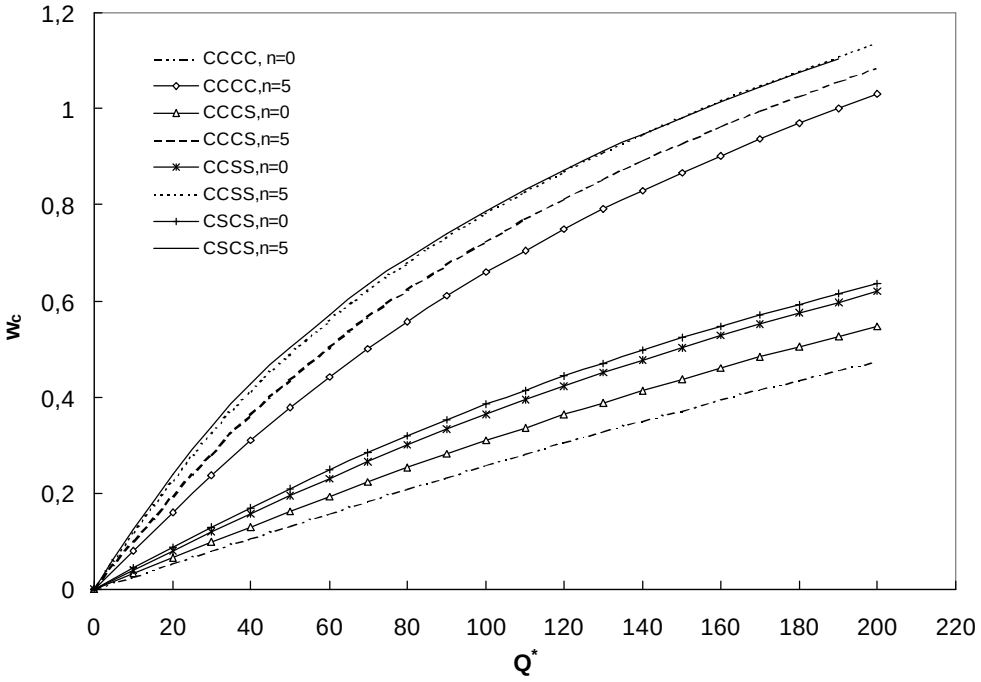

Fig.8. Effect of boundary conditions on the transverse central deflection w_c of the clamped FGM plate $(a/h=20)$ under uniform lateral loading.

Figure 9 depicts the effect of volume fraction exponent n on the linear and nonlinear dynamic displacement responses of the moderately thick $(a/h=20)$ FGM plate with clamped boundary conditions on all the edges under uniform step loading. The maximum amplitude of motion is higher in case of linear response than nonlinear response for all the values of n and it increases with n for linear as well as nonlinear responses. The difference in the maximum amplitude of motion between linear and nonlinear responses increases with an increase in n value and the difference is highest when the plate is fully made of aluminum and lowest when the plate is fully made of alumina.

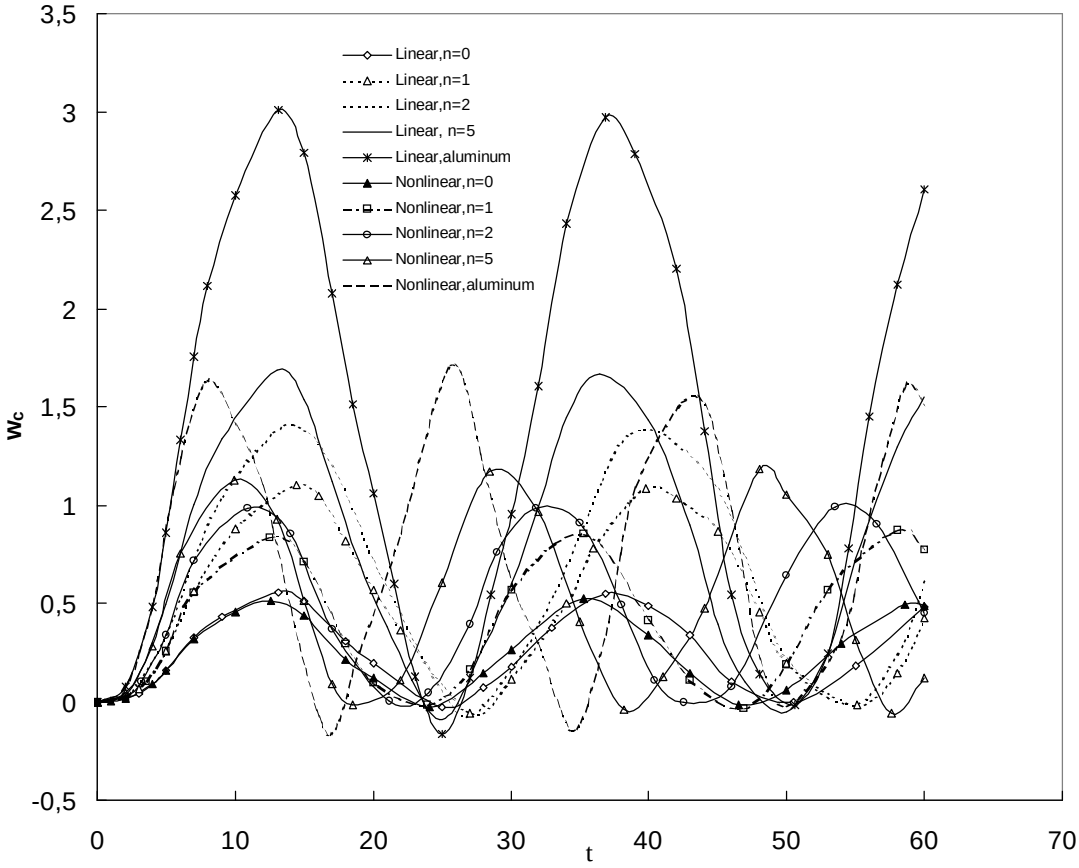

Fig.9. Effect of volume fraction exponent n on dynamic transverse displacement response of the clamped FGM plate $(a/h = 20)$ under uniform step loading $(Q^* = 100)$.

The effect of plate span to thickness ratio a/h on the nonlinear dynamic central displacement response of the clamped FGM plate for volume fraction exponent n equal to 0 and 2 is shown in Fig.10. It is observed that for both the values of n the maximum amplitude of the motion decreases slightly with an increase in a/h, but decrease in the frequency of motion with an increase in a/h values is significant. The effect of volume fraction exponent n on the central moment M_x^* of the clamped FGM plate $(a/h = 20)$ under uniform step loading is shown in Fig.11. It is observed that the moment M_x^* remains almost positive for $n = 0$, 1 and 2 and its value is almost same for $n = 1$ and 2, but for fully aluminum plate the value of M_x^* changes its nature and it is higher than any other value of the volume fraction exponent n, indicating the greater influence of n which changes the stiffness of the FGM plate.

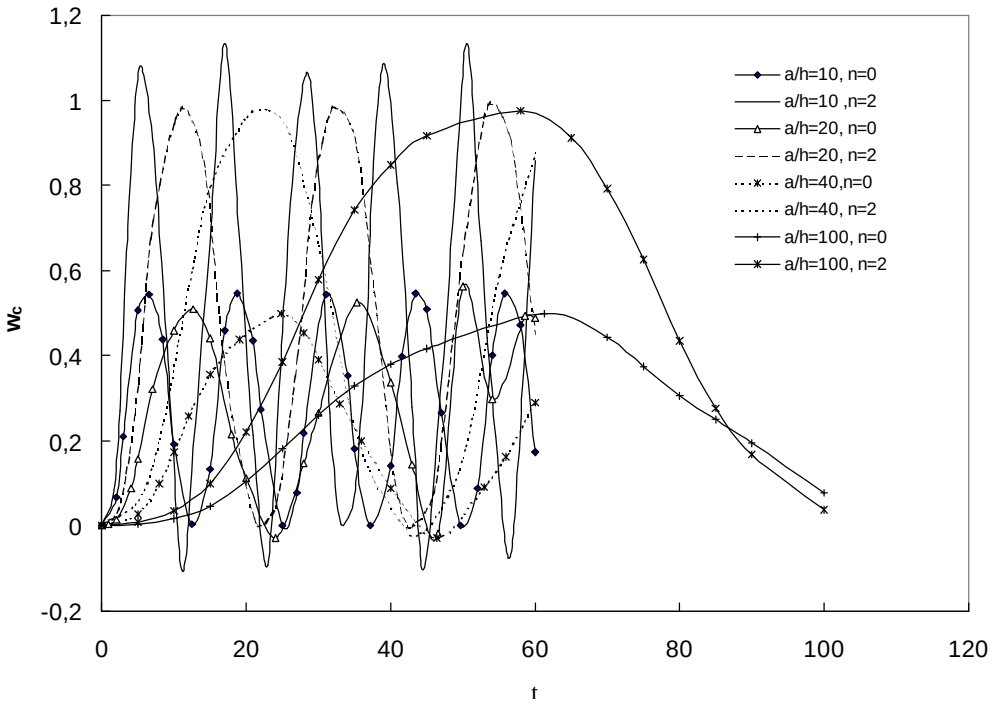

Fig.10. Effect of plate span to thickness ratio a/h on nonlinear dynamic transverse displacement response of the clamped FGM plate under uniform step loading $\left(Q^* = 100\right)$.

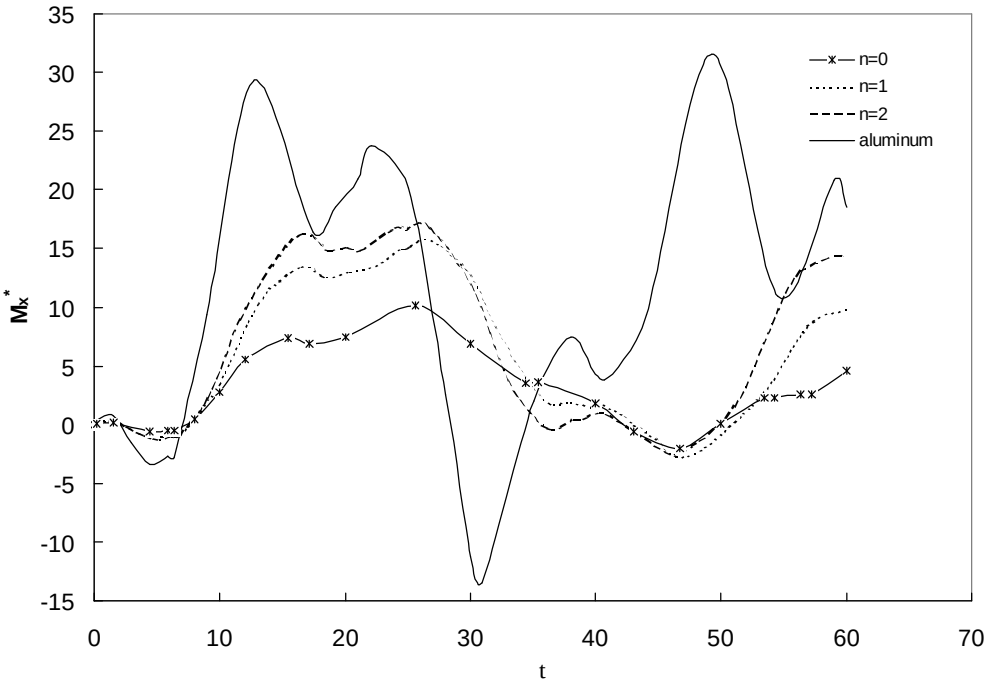

Fig.11. Variation of moment M_x^* at the center of the clamped FGM plate $\left(a/h = 20\right)$ under uniform step loading $\left(Q^* = 100\right)$ for different values of *n*.

5. Concluding remarks

The nonlinear static and dynamic responses of the functionally graded materials plate with non-classical boundary conditions are obtained, explicitly. The effect of volume fraction exponent on the static and dynamic transverse displacement responses is obtained, which may be useful for determining the volume fraction of the materials for a desired response. Analysis results indicate that the volume fraction exponent has a significant effect on the response of the plate and with an increase in the value of the volume fraction exponent up to two, the transverse deflection increases significantly in both the static and dynamic loading cases, indicating that the plate stiffness reduces with an increase in *n*. The effect of volume fraction exponent is similar for thin and moderately thick plates. The present solution methodology can be extended for obtaining the buckling and post-buckling response of the FGM plates under thermal and thermomechanical loading, which may be helpful for optimal design of the FGM plates under different loading conditions.

Acknowledgments

The authors gratefully acknowledge the financial support of the National Science Council of Taiwan, Republic of China (Contract Nos. NSC 90-2212-E-035-004, 90-2745-P-035-004, and 91-2212-E-035-008).

Nomenclature

a, b, h – plate dimensions
A_{ij}, B_{ij}, D_{ij} – in-plane, coupling, bending stiffnesses of the plate, respectively
CCCC – all edges clamped
CCCS – three edges clamped and one edge simply supported
CCSS – two opposite edges clamped and two simply supported
CSCS – two adjacent edges clamped and two simply supported
E_c, E_m – modulus of elasticity of ceramic and metal, respectively
n – volume fraction exponent
N^*, M^*, Q^* – non dimensional in-plane force, moment, and transverse load at centre
U, V, W – displacement of plates at any point in *x, y, z* directions, respectively
u_0, v_0, w_0 – displacement of plates at mid plane in *x, y, z* directions, respectively
w_c – non dimensional central displacement
ρ_c, ρ_m – mass density of ceramic and metal, respectively
ν – Poisson's ratio
θ_x, θ_y – slopes in *xz, yz* planes, respectively
τ – non-dimensional time

References

Chia C.Y. (1988): *Geometrically nonlinear behaviour of composite plates: A review.* – ASME, Appl. Mech. Rev., vol.41, No.12, pp.439-454.

Evans D.J. and Murphy C.P. (1981): *The solution of biharmonic equation in a rectangular region by Chebyshev series.* – Comput. Methods Appl. Mech. Eng., vol.27, pp.81-99.

Finot M. and Suresh S. (1996): *Small and large deformation of thick and thin film multilayers: effects of layer geometry, plasticity and compositional gradients.* – J. Mech. Phys. Solids., vol.44, No.5, pp.683-721.

Fox L. and Parker I.B. (1968): *Chebyshev polynomials in numerical analysis.* – London: Oxford University Press.

Houbolt J.C. (1950): *A recurrence matrix solution for the dynamic response of the elastic Aircraft.* – J. Aero. Sci., vol.17, pp.540-550.

Koizumi M. (1993): *The concept of FGM.* – Ceram. Trans., vol.34, No.1, pp.3-10.

Lin C.H. and Jen M.H.R. (2003): *Analysis of laminated anisotropic cylindrical shell by Chebyshev collocation method.* – J. Applied Mechanics, ASME, vol.70, pp.391-403.

Loy C.T., Lam K.Y. and Reddy J.N. (1999): *Vibration of functionally graded cylindrical Shells.* – Int. J. Mech. Sci., vol.41, No.3, pp.309-324.

Ma L.S. and Wang T.J. (2003): *Nonlinear bending and post-buckling of a functionally graded circular plate under mechanical and thermal loadings.* – Int. J. Solids Struct., vol.40, pp.3311-3330.

Nath Y. and Shukla K.K. (2001): *Nonlinear transient analysis of moderately thick laminated composite plates.* – J. Sound Vib., vol.247, No.3, pp.509-526.

Pradhan S.C., Loy C.T., Lam K.Y. and Reddy J.N. (2000): *Vibration characteristics of functionally graded cylindrical shells under various boundary conditions.* – Appl. Acoust., vol.61, No.1, pp.111-129.

Praveen G.N. and Reddy J.N. (1998): *Nonlinear transient thermoelastic analysis of functionally graded ceramic-metal plates.* – Int. J. Solids Struct., vol.35, No.33, pp.4457-4476.

Reddy J.N. (2000): *Analysis of functionally graded plates.* – Int. J. Numer. Meth. Eng., vol.47, pp.663-684.

Reddy J.N. and Chin C.D. (1998): *Thermomechanical analysis of functionally graded cylinders and plates.* – J. Thermal Stresses, vol.21, pp.593-626.

Sathyamoorthy M. (1987): *Nonlinear vibration analysis of plates: A review and survey of current developments.* – ASME, Appl. Mech. Rev., vol.40, pp.1553-1561.

Shukla K.K., Chen J.M. and Huang J.H. (2004): *Nonlinear dynamic analysis of composite laminated plates containing spatially oriented short fibers.* – Int. J. Solids Struct., vol.41, pp.365-384.

Turvey G.J. and Osman M.Y. (1990): *Elastic large deflection analysis of isotropic rectangular plates.* – Int. J. Mech. Sci., vol.32, No.4, pp.315-328.

Tauchert T.R. (1991): *Thermally induced flexure, buckling and vibration of plates.* – ASME, Appl. Mech. Rev., vol.44, No.8, pp.347-360.

Vel S.S. and Batra R.C. (2002): *Exact solution for thermoelastic deformations of functionally graded thick rectangular plates.* – AIAA J., vol.40, No.7, pp.1421-1433.

Vel S.S. and Batra R.C. (2003): *Three-dimensional analysis of transient thermal stresses in functionally graded plates.* – Int. J. Solids Struct., vol.40, pp.7181-7196.

Yang J. and Shen H.-S. (2003): *Nonlinear bending analysis of shear deformable functionally graded plates subjected to thermo-mechanical loads under various boundaryconditions.* – Composites: Part B, vol.34, pp.103-115.

Zhong Z. and Shang E.T. (2003): *Three-dimensional exact analysis of a simply supported functionally gradient piezoelectric plate.* – Int. J. Solids Struct., vol.40, pp.5335-5352.

APPENDIX

The matrices defined in the governing Eq.(2.11) are defined as

$$L_{a1}=\begin{bmatrix} 1 & 0 & 0 & \frac{B_{11}}{hA_{11}} & 0 \\ 0 & \frac{A_{66}}{A_{22}} & 0 & 0 & \frac{B_{66}}{hA_{22}} \\ 0 & 0 & \frac{A_{55}}{A_{22}} & 0 & 0 \\ \frac{hB_{11}}{D_{11}} & 0 & 0 & 1 & 0 \\ 0 & \frac{hB_{66}}{D_{22}} & 0 & 0 & \frac{D_{66}}{D_{22}} \end{bmatrix}, \tag{A1}$$

$$L_{a2}=\begin{bmatrix} \frac{\lambda^2 A_{66}}{A_{11}} & 0 & 0 & \frac{\lambda^2 B_{66}}{hA_{11}} & 0 \\ 0 & \lambda^2 & 0 & 0 & \frac{B_{66}}{hA_{22}} \\ 0 & 0 & \frac{\lambda^2 A_{44}}{A_{22}} & 0 & 0 \\ \frac{h\lambda^2 B_{66}}{D_{11}} & 0 & 0 & \frac{\lambda^2 D_{66}}{D_{11}} & 0 \\ 0 & \frac{h\lambda^2 B_{22}}{D_{22}} & 0 & 0 & \lambda^2 \end{bmatrix}, \tag{A2}$$

$$L_{a3}=\begin{bmatrix} 0 & \frac{\lambda(A_{12}+A_{66})}{A_{11}} & 0 & 0 & \frac{\lambda(B_{12}+B_{66})}{hA_{11}} \\ \frac{\lambda(A_{12}+A_{66})}{A_{22}} & 0 & 0 & \frac{\lambda(B_{12}+B_{66})}{hA_{22}} & 0 \\ 0 & 0 & 0 & 0 & 0 \\ 0 & \frac{h\lambda(B_{12}+B_{66})}{D_{11}} & 0 & 0 & \frac{\lambda(D_{12}+D_{66})}{D_{11}} \\ \frac{h\lambda(B_{12}+B_{66})}{D_{22}} & 0 & 0 & \frac{\lambda(D_{12}+D_{66})}{D_{22}} & 0 \end{bmatrix}, \tag{A3}$$

$$\boldsymbol{L}_{a4}=\begin{bmatrix} 0 & 0 & 0 & 0 & 0 \\ 0 & 0 & 0 & 0 & 0 \\ 0 & 0 & 0 & \dfrac{A_{55}a}{2A_{22}h} & 0 \\ 0 & 0 & -\dfrac{ahA_{55}}{2D_{11}} & 0 & 0 \\ 0 & 0 & 0 & 0 & 0 \end{bmatrix}, \quad \boldsymbol{L}_{a4}=\begin{bmatrix} 0 & 0 & 0 & 0 & 0 \\ 0 & 0 & 0 & 0 & 0 \\ 0 & 0 & 0 & 0 & \dfrac{\lambda aA_{44}}{2hA_{22}} \\ 0 & 0 & 0 & 0 & 0 \\ 0 & 0 & -\dfrac{ah\lambda A_{44}}{2D_{22}} & 0 & 0 \end{bmatrix}, \tag{A4}$$

$$\boldsymbol{L}_{a6}=\begin{bmatrix} 0 & 0 & 0 & 0 & 0 \\ 0 & 0 & 0 & 0 & 0 \\ 0 & 0 & 0 & 0 & 0 \\ 0 & 0 & 0 & -\dfrac{a^2A_{55}}{4D_{11}} & 0 \\ 0 & 0 & 0 & 0 & -\dfrac{a^2A_{44}}{4D_{22}} \end{bmatrix}. \tag{A5}$$

$\boldsymbol{L}_{b1}$, $\boldsymbol{L}_{b2}$, $\boldsymbol{L}_{b3}$, $\boldsymbol{L}_{c1}$, $\boldsymbol{L}_{c2}$ and $\boldsymbol{L}_{c3}$ are 5×5 matrices and all elements are zero except

$$\boldsymbol{L}_{b1}(1,3)=\frac{2h}{a}w_{,x}, \qquad \mathbf{L}_{b1}(2,3)=\frac{2\lambda hA_{66}}{A_{22}a}w_{,y},$$

$$\mathbf{L}_{b1}(3,3)=\frac{2h}{A_{22}a}\left(A_{11}u_{,x}+\lambda A_{12}v_{,y}\right)+\frac{2}{A_{22}a}\left(B_{11}\theta_{x,x}+\lambda B_{12}\theta_{y,y}\right),$$

$$\boldsymbol{L}_{b1}(4,3)=\frac{2h^2B_{11}}{D_{11}a}w_{,x}, \qquad \boldsymbol{L}_{b1}(5,3)=\frac{2\lambda h^2B_{66}}{\beta D_{22}}w_{,y},$$

$$\boldsymbol{L}_{b2}(1,3)=\frac{2\lambda^2hA_{66}}{A_{11}a}w_{,x}, \qquad \boldsymbol{L}_{b2}(2,3)=\frac{2\lambda^3h}{a}w_{,y}, \tag{A6}$$

$$\mathbf{L}_{b2}(3,3)=\frac{2\lambda^2h}{A_{22}a}\left(A_{12}u_{,x}+\lambda A_{22}v_{,y}\right)+\frac{2\lambda^2}{A_{22}a}\left(B_{12}\theta_{x,x}+\lambda B_{22}\theta_{y,y}\right),$$

$$\boldsymbol{L}_{b2}(4,3)=\frac{2h^2\lambda^2B_{66}}{D_{11}a}w_{,x}, \qquad \boldsymbol{L}_{b2}(5,3)=\frac{2h^2\lambda^3B_{22}}{D_{22}a}w_{,y},$$

$$\mathbf{L}_{b3}(1,3)=\frac{2\lambda^2h(A_{12}+A_{66})}{A_{11}a}w_{,y}, \qquad \boldsymbol{L}_{b3}(2,3)=\frac{2\lambda h(A_{12}+A_{66})}{A_{22}a}w_{,x},$$

$$\mathbf{L}_{b3}(3,3)=\frac{4\lambda h}{A_{22}a}\left(\lambda A_{66}u_{,y}+A_{66}v_{,x}\right)+\frac{4\lambda}{A_{22}a}\left(\lambda B_{66}\theta_{x,y}+B_{66}\theta_{y,x}\right),$$

$$\boldsymbol{L}_{b3}(4,3)=\frac{2h^2\lambda^2\left(B_{12}+B_{66}\right)}{D_{11}a}w_{,y}, \qquad \boldsymbol{L}_{b3}(5,3)=\frac{2h^2\lambda\left(B_{12}+B_{66}\right)}{D_{22}a}w_{,x},$$

$$\boldsymbol{L}_{c1}(3,3)=\frac{2h^2}{A_{22}a^2}\left\{A_{11}\left(w_{,x}\right)^2+\lambda^2A_{12}\left(w_{,y}\right)^2\right\}, \tag{A6}$$

$$\boldsymbol{L}_{c2}(3,3)=\frac{2\lambda^2h^2}{A_{22}a^2}\left\{A_{12}\left(w_{,x}\right)^2+\lambda^2A_{22}\left(w_{,y}\right)^2\right\},$$

$$\boldsymbol{L}_{c3}(3,3)=\frac{8\lambda^2h^2A_{66}}{a^2}w_{,x}w_{,y},$$

$$\mathbf{L}_{d1}=\begin{bmatrix} \dfrac{A_{22}}{A_{11}} & 0 & 0 & \dfrac{A_{22}Rh}{D_{22}Ph} & 0 \\ 0 & 1 & 0 & 0 & \dfrac{R}{Ph} \\ 0 & 0 & 1 & 0 & 0 \\ \dfrac{A_{22}Rh}{D_{11}P} & 0 & 0 & \dfrac{A_{22}I}{D_{11}P} & 0 \\ 0 & \dfrac{A_{22}Rh}{D_{22}P} & 0 & 0 & \dfrac{A_{22}I}{D_{22}P} \end{bmatrix} \tag{A7}$$

where P, R and I are the normal, coupled normal rotary and rotary inertia coefficients and defined as

$$\left(P,R,I\right)=\int_{-h/2}^{h/2}\rho(z)\left(1,z,z^2\right)dz. \tag{A8}$$

The non-dimensional parameters appearing in the foregoing equations are defined as

$$\lambda=\frac{a}{b}, \qquad x=\frac{2X}{a}, \qquad y=\frac{2Y}{b}, \qquad u=\frac{u_0}{h}, \qquad v=\frac{v_0}{h}, \qquad w=\frac{w_0}{h},$$

$$N_x^*=\frac{N_xa}{A_{11}h}, \qquad N_y^*=\frac{N_ya}{A_{22}h}, \qquad N_{xy}^*=\frac{N_{xy}a}{A_{66}h}, \qquad M_x^*=\frac{M_xa^2}{D_{11}h}, \tag{A9}$$

$$M_y^*=\frac{M_ya^2}{D_{22}h}, \qquad M_{xy}^*=\frac{M_{xy}a^2}{D_{66}h}, \qquad \tau=t\sqrt{\frac{4A_{22}}{Pa^2}}.$$

Received: November 4, 2004
Revised: February 25, 2005